Fast, Accurate and Convergent Tangent Estimation on Digital Contours

Jacques-Olivier Lachaud, Anne Vialard, and François de Vieilleville

LaBRI, Univ. Bordeaux 1, 351 cours de la Libération, 33405 Talence Cedex, France
{lachaud,vialard,devieill}@labri.fr

Abstract. This paper presents a new tangent estimator to digitized curves based on digital line recognition. It outperforms existing ones on important criteria while keeping the same computation time: accuracy on smooth or polygonal shapes, isotropy, preservation of inflexion points and convexity, asymptotic behaviour. Its asymptotic convergence (sometimes called *multigrid convergence*) is proved in the case of convex shapes.

1 Introduction

In this paper, we address the problem of tangent estimation along contours of digitized 2D objects. Tangent estimation is useful for estimating many geometric quantities and has also many applications. For instance, the length of a digital contour is accurately estimated from tangents by integration [3, 18]. Derivating the orientation of the tangent provides an estimation of the curvature [18, 22, 23]. The previous geometric parameters are used in classical pattern recognition applications. They also define the internal energies of discrete deformable models [15]. When rendering 3D digitized objects, the normal vector field can be estimated from tangent directions along slice contours [16, 18].

When trying to estimate geometric properties of digitized objects, we face the issue that infinitely many shapes have the same digitization: there is no good approximation since there is no reference shape. Other hypotheses are thus required. The common assumption is that the original continuous object has some "natural" properties such as: compactness (not a fractal), bounded curvature, sometimes piecewise linear geometry (i.e. polygon). Therefore we restrict the class of shapes we are interested in. Discrete boundaries will come from the digitization of continuous shapes composed of polygonal parts and of smooth parts with bounded curvature.

Many tangent estimators are based on a finite set of $2k+1$ curve points around the point of interest. Matas *et al.* [19] compute the tangent direction as the median direction of the vectors linking the processed point to the k next points and to the k previous points on the curve. Worring describes several methods for computing the tangent orientation in a survey on curvature estimation [23]. Among them a method by Anderson and Bezdek [1] defines the tangent at a point as a real line segment fitting the $2k+1$ neighbouring points by minimizing their squared distances to the line. Lenoir [18] uses a recursive gaussian filter to obtain a local mean orientation of the curve.

Although interesting in some contexts, all the previous methods require an external parameter, the size of the "computation window", often fixed globally by the user. One consequence is that the tangent estimation provided by these methods cannot converge asymptotically toward the continuous value as the digitization resolution increases: the computation scale is defined globally and is not adapted to the local shape geometry. These tangent estimators are said to be *non convergent*. This paper is concerned with the design of discrete tangent estimators that are convergent (or *multigrid convergent* for some authors [12, 3]).

The convergence of some global geometric estimators in the plane and particularly of length estimators has been studied in several works [13, 2, 12]. They proved that the shape perimeter, the shape area, its center of gravity, its orientation and its elongation can be estimated more and more precisely as the resolution increases. There are very few results about the convergence of local geometric estimators. Some elements about the convergence (or non-convergence) of tangent and curvature estimation can be found in [4, 2, 6].

Although these studies do not prove the convergence of a local discrete geometric estimator, they give hints as how to design convergent tangent estimators. We will therefore consider tangent estimators based on digital straight segment extraction [22, 10, 16]: digital straight segments along digitized curves naturally define a window, whose size is dependent of the local shape geometry. In these works, the discrete tangent is defined as a longest digital straight segment corresponding to the digital curve around the point of interest. The tangent size thus grows as the curvature decreases. It is well known that this estimation is exact when the shape is a half-plane. These discrete tangent estimators thus seem to be good candidates to design a convergent tangent estimator. This point is however not straightforward. It is shown in [14] that even smooth and regular curves frequently contain an infinite set of points called critical points where the symmetric tangent estimator (see Section 2 for a definition) fails at giving a tangent estimation that converges toward the expected value when the resolution increases.

We propose in this paper a new discrete tangent estimator which is shown to be asymptotically convergent. An upper bound on the average rate of convergence is also given. Furthermore, it is accurate at low scale with low deviation and maximum error and has good isotropic properties. Its computation cost depends linearly on the number of curve points, i.e. it is optimal. Other interesting intermediary properties are demonstrated in this paper: the length of maximal segments is not bounded on finer and finer digitization of smooth curves, maximal segments are related to digital convexity.

The paper is organized as follows. In Section 2, we recall the existing definitions of discrete tangents and compare qualitatively their advantages and drawbacks. We then present the new tangent estimator, called λ-*MST*, that takes the best out of the existing ones. This estimator is based on the set of maximal digital straight segments going through the point of interest. We prove in Section 3 that it identifies convex and concave parts of the shape and behaves accordingly. In Section 4, we prove in the case of convex shapes the asymptotic convergence of tangent estimators defined by the direction of maximal segments and, consequently, the convergence of λ-MST. In Section 5 we show that the computational complexity of λ-MST is equivalent to the other existing estimators both locally and globally for the whole curve. Section 6 is devoted to an experimental evaluation of λ-MST which is compared to the other discrete tangent estimators. We have checked the following points: tangent estimation on smooth and straight parts of the shape, sharp corner recognition, isotropy, mean and maximal asymptotic error with different shapes. Experiments confirm that the λ-MST has the best behaviour in most practical cases.

2 Estimating tangent with digital straight segments

This section recalls some standard discrete geometry notions, presents tangent estimators based on digital straight segment recognition, and propose a new tangent estimator.

We restrict our study to the geometry of 4-connected digital curves. Indeed, a digital object is a set of pixels and its boundary when seen as a collection of pointels and linels is a 4-connected curve. Besides this work may easily be adapted to 8-connected curves since it relies on discrete straight segment recognition. We introduce some notations to get homogeneous definitions of existing tangent estimators based on digital straight lines. In the remaining of the paper, the digital curve is denoted by C. Its points (C_k) are assumed to be indexed from 0 to $N-1$. A set of successive points of C ordered increasingly from index i to j will be conveniently denoted by $C_{i,j}$.

2.1 Standard line, digital straight segment, maximal segments

Definition 1. *The set of points (x, y) of the digital plane verifying $\mu \leq ax-by < \mu + |a| + |b|$, with a, b and μ integer numbers, is called the* standard line *with slope a/b and shift μ [21].*

The *standard lines* are the 4-connected discrete lines. As we will see later, all discrete tangents are defined as particular connected subset of standard lines included in 4-connected digital curves.

Since the tangent is a local property of the curve, we can always assume that we look at a restricted part of C, where the indices are totally ordered (the curve can be re-indexed differently so that its indices are totally ordered on the subpart of interest). The following definition is thus valid.

Definition 2. *We say that a set of consecutive points $C_{i,j}$ of the digital curve C is a* digital straight segment (DSS) *iff there exists a standard line (a, b, μ) containing them. Any DSS defines an angle between its carrying standard line and the x-axis (in $[0; 2\pi[$ since a DSS is oriented). This angle will be called later on the* direction of the DSS.

The predicate *"$C_{i,j}$ is a DSS"* is denoted by $S(i,j)$. When $S(i,j)$, we denote by $D(i,j)$ the characteristics associated with the digital straight segment [7]: the characteristics (a,b,μ) of the standard line containing all the points $C_{i,j}$, the principal upper and lower leaning points U_m, U_M, L_m and L_M. Let us recall that an upper leaning point verifies $ax - by = \mu$, i.e. it belongs to the upper leaning line, while a lower leaning point belongs to the lower leaning line of equation $ax - by = |a| + |b| + \mu - 1$. We denote by U_m (respectively by U_M) the upper leaning point of minimum (resp. maximum) abscissa and by L_m (respectively by L_M) the lower leaning point of minimum (resp. maximum) abscissa. The previous definitions and notations are illustrated in Figure 1.

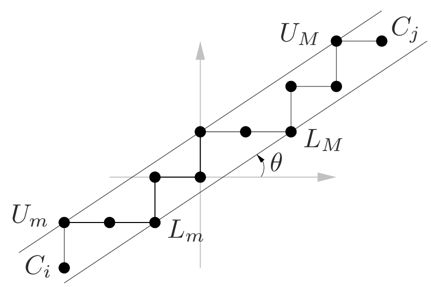

Fig. 1. Digital straight segment of characteristics $(a,b,\mu) = (2,3,-3)$ and direction θ.

The first index j, $i \leq j$, such that $S(i,j)$ and $\neg S(i,j+1)$ is called the *front* of i. The map associating any i to its front is denoted by F. Symmetrically, the first index i such that $S(i,j)$ and $\neg S(i-1,j)$ is called the *back* of j and the corresponding mapping is denoted by B. We get the following obvious relations.

Proposition 1. *(i)* $\forall i \leq i' \leq j' \leq j, S(i,j) \Rightarrow S(i',j')$*;*
(ii) F *and* B *are locally increasing;*
(iii) $F \circ B \circ F = F$ and $B \circ F \circ B = B$.

The definition of maximal segments will be central for estimating tangents. They form the longest possible DSS in the curve. They are used for polygonizing a digital curve into the minimum number of segments [11], for defining discrete convexity [8], for proving the convergence or the non-convergence of discrete geometric estimators [6]. Proposition 1 allows us to give four equivalent definitions of maximal segments:

Definition 3. *Any set of points* $C_{i,j}$ *is called a* maximal segment (MS) *iff any of the following equivalent characterizations holds: (1)* $S(i,j)$ *and* $\neg S(i,j+1)$ *and* $\neg S(i-1,j)$*, (2)* $B(j) = i$ *and* $F(i) = j$*, (3)* $\exists k, i = B(k)$ *and* $j = F(B(k))$*, (4)* $\exists k', i = B(F(k'))$ *and* $j = F(k')$*.*

Figure 2 illustrates this definition.

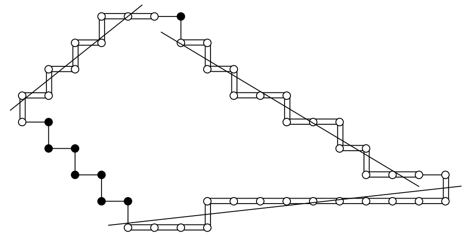

Fig. 2. Three non-overlapping maximal segments (in white) on a digital contour.

Any contour point obviously belongs to at least one maximal segment. The set of all maximal segments thus covers a digital contour. This notion was already used for example by Feschet and Tougne under the name *tangential cover* [10]. It is illustrated in Figure 3.

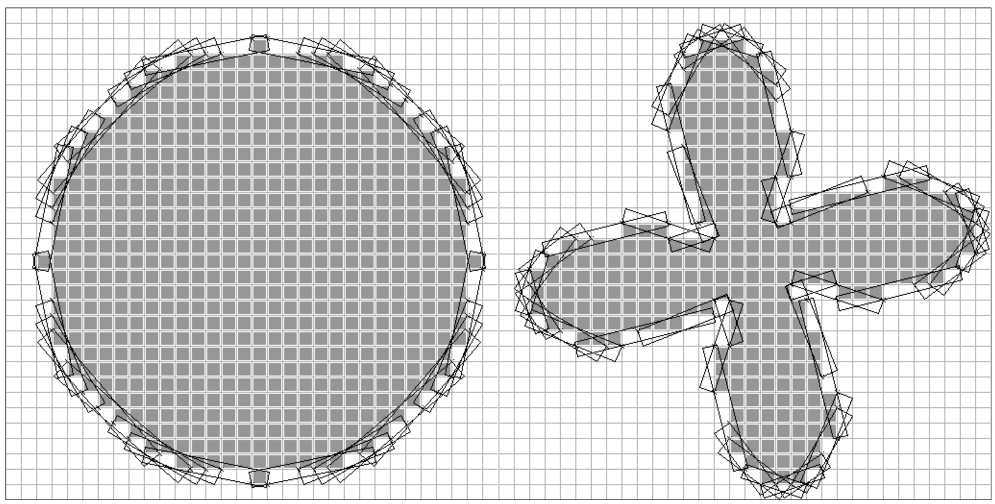

Fig. 3. Tangential cover of a digital contour. Each maximal segment is represented by its rectangular bounding box. Left : the digital shape is a disk of radius 14. Right : the digital shape is a flower with important curvature variations and inflexion points.

2.2 Discrete tangents

Based on local DSS recognition, several tangent estimators at a digital curve point have been proposed. Their quality is to adapt the computation window to the local shape of the curve. Exact tangent estimation for digitizations of straight lines can thus be achieved. They all try to make the right balance between longest and most centered DSS around the point of interest.

Definition 4. *The following DSS may be defined around any point C_k of the digital curve C. They correspond to the notion of* discrete tangent *(see Fig. 4).*

– *The DSS $C_{k-l,k+l}$ with $S(k-l, k+l)$ and $\neg S(k-l-1, k+l+1)$ is called the* symmetric tangent (ST) at C_k *[16].*
– *The maximal segment with biggest indices that includes the symmetric tangent at C_k is called the* Feschet-Tougne tangent (FTT) at C_k *[10].*
– *The* extended tangent (ET) at C_k *includes the symmetric tangent $C_{k-l,k+l}$ but may be extended in the two following cases: (i) if $S(k-l, k+l+1) \wedge \neg S(k-l-1, k+l)$ then it is extended forward as the maximal segment $C_{k-l,F(k-l)}$, (ii) if $S(k-l-1, k+l) \wedge \neg S(k-l, k+l+1)$ then it is extended backward as the maximal segment $C_{B(k+l),k+l}$.*
– *The* forward half-tangent at C_k *is the DSS $C_{k,F(k)}$ and the* backward half-tangent at C_k *is the DSS $C_{B(k),k}$. The* median half-tangent (HT) at C_k *is the arithmetical line median to the two half-tangents.*

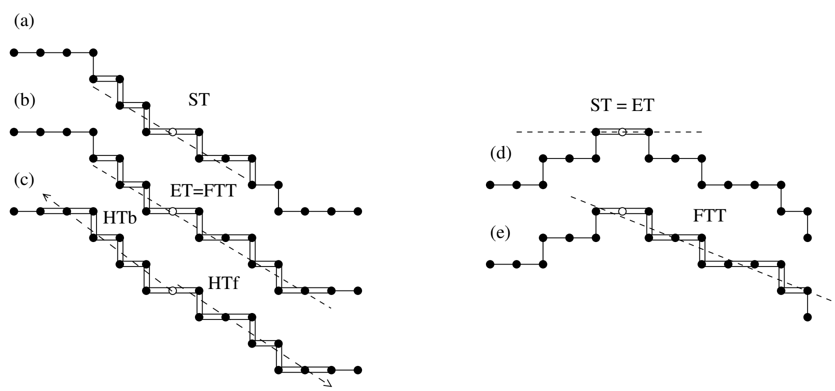

Fig. 4. Illustration of different definitions of a discrete tangent. The point of interest is represented in white as well as the set of contour edges of the discrete tangent. (a) Symmetric Tangent. (b) Extended Tangent which is equivalent on this example to the Feschet-Tougne Tangent. (c) forward and backward Half-Tangents. Subfigures (d) and (e) emphasize the possible ambiguity in the definition of FTT: balanced tangent for ET and ST versus arbitrarily unbalanced tangent for FTT.

The preceding discrete tangent definitions, except for the FTT, are independent of the orientation chosen for the curve (Fig. 4*d-e*). ET can be seen as an unambiguous version of FTT. Both FTT and ET are local longest DSS, to the expense of a loss of localization around the point. FTT and ET tend to polygonalize the digital curve even for underlying smooth shapes.

On the other hand, ST and HT have a very good localization around the point (perfectly centered for ST). However they both may have a bad behavior on even very regular shapes (e.g. at the points where a circle with integer radii touches the axes). They may also not locate accurately convex or concave parts of the curve. This point will be detailed in Section 3. Note that HT is also used for estimating the curvature [2].

In the next section, we construct a new tangent estimator which combines the qualities of the other ones: related to maximal segments as FTT and ET; computation window identical to HT; significant position of the point wrt the DSS surrounding it as ST; unambiguous definition.

2.3 Tangent estimation based on maximal segments

The new tangent estimator depends on the set of maximal segments that goes through a point of the digital curve. This set is called the *pencil of maximal segments* around the point of interest. As noted by Feschet and Tougne [10], several successive points may have the same pencil. Therefore the tangent estimator takes also into account the position of the point within the pencil. More specifically, the point has a given eccentricity wrt each maximal segments. The tangent direction is estimated by a combination of the direction of each maximal segment weighted by the eccentricity.

We index all the maximal segments of the curve by increasing indices: $M_i = C_{m_i,n_i}$ with $F(m_i) = n_i$ and $B(n_i) = m_i$. From characterizations (3) and (4) of the definition of maximal segment (Definition 3), any DSS $C_{i,j}$ and hence any point belongs to at least two maximal segments (possibly identical) $C_{B(j),F(B(j))}$ and $C_{B(F(i)),F(i)}$. Therefore, the *pencil of maximal segments* $\mathcal{P}(k) = \{M_i, k \in M_i\}$ around any point C_k is never empty. We denote by θ_i the direction of the DSS M_i. In the remaining of the paper, λ is a mapping from $[0, 1]$ to $\mathbb{R}^+$ with $\lambda(0) = \lambda(1) = 0$ and $\lambda > 0$ elsewhere.

The *eccentricity* $e_i(k)$ of a point C_k wrt a maximal segment M_i is its relative position between the extremeties of M_i:

$$e_i(k) = \begin{cases} \frac{\|C_k - C_{m_i}\|_1}{L_i} = \frac{k-m_i}{L_i} & \text{if } M_i \in \mathcal{P}(k) \\ 0 & \text{otherwise} \end{cases}, \text{ with } L_i = \|C_{n_i} - C_{m_i}\|_1. \quad (1)$$

Given a point on a maximal segment, the more its eccentricity is close to $\frac{1}{2}$ the more it is centered (see Fig. 5).

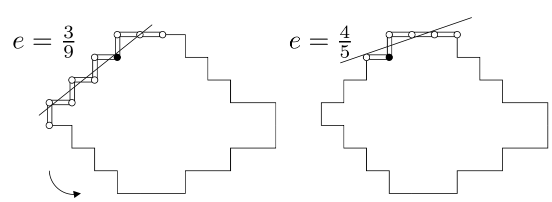

Fig. 5. Computation of the eccentricity e of a contour point (in black) wrt a maximal segment (in white).

Definition 5. *The* λ-maximal segment tangent direction at point C_k (λ-MST) *is then defined as a weighted combination of the directions of the surrounding maximal segments:*

$$\hat{\theta}(k) = \frac{\sum_{i \in \mathcal{P}(k)} \lambda(e_i(k))\theta_i}{\sum_{i \in \mathcal{P}(k)} \lambda(e_i(k))} = \frac{\sum_i \lambda(e_i(k))\theta_i}{\sum_i \lambda(e_i(k))}. \tag{2}$$

Considering the properties of the eccentricity and the non-emptyness of pencils, this value is always defined and may be computed locally.

The preceding notion is extended to any real value k in $[0, N[$. It is enough to consider k as the curvilinear parameterization of the 4-connected contour. Any non-integer value of k corresponds to a real point on the straight line linking $C_{\lfloor k \rfloor}$ and $C_{\lceil k \rceil}$. When λ is continuous, the angle $\hat{\theta}(k)$ is continuous too and a length estimator may be derived from it [17].[1] The length of the curve can be estimated by simple integration of this local measure. Cœurjolly and Klette have reported that this method of length evaluation gives very good results [3].

3 Local convexity or concavity

One can expect that a tangent estimator preserves the inflexion points, i.e. it detects them without creating false ones. It is not the case for ST or HT. Figure 6 shows an example of incorrect behaviour of ST. The digitized contour is here a circular arc. The quadrant change around the point of interest implies that the symmetric tangent has a slope greater than the slope of the following contour points. In other words, the ST estimator has detected a concavity on a disk.

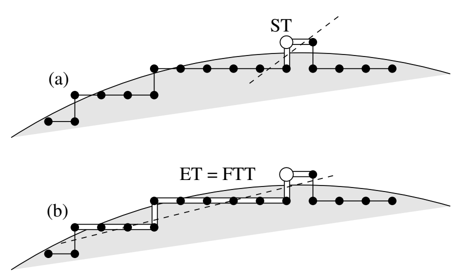

Fig. 6. Tangent estimation along the digitization of a circular shape. False concavity detected by ST (a) versus correct straight line for ET and FTT (b).

Definition 6. *The digital curve C is oriented counterclockwise wrt the discrete object it bounds. C is* locally convex (resp. concave) at point C_k *iff the angles* (θ_i)

[1] For instance, if h is the grid step, the elementary length mat be given by $\hat{l}(k) = \frac{h}{|cos(\hat{\theta}(k))|+|sin(\hat{\theta}(k))|}$.

of the sorted segments of $\mathcal{P}(k)$ is an nondecreasing sequence (resp. nonincreasing sequence). (Angles are brought back in $]-\pi,\pi[$ relatively to the first one.)

This local version of convexity is related to traditional convexity: the digitization of a convex shape is digitally convex for a fine enough grid step [9]; and it is proven in [20] (Theorem 4.1) that a digitally convex shape satisfies the local convexity property everywhere.

We say that a tangent estimator to a digital curve satisfies the *convexity/concavity property* iff the estimated tangent direction is nondecreasing (resp. nonincreasing) on every connected subset where the curve is locally convex (resp. concave). This property holds for ET and FTT but does not hold for ST and HT (e.g. see Fig. 6 or Fig. 16). For λ-MST, it depends on the function λ as indicated below.

Theorem 1. *If λ is differentiable on $]0,1[$, then the λ-MST estimator satisfies the convexity/concavity property iff $\frac{d}{dt}(t\frac{\lambda'}{\lambda}(t)) \leq 0$ and $\frac{d}{dt}((1-t)\frac{\lambda'}{\lambda}(t)) \leq 0$ hold on this interval.*

The proof is given in appendix. It is easy to check that functions with a bell shape satisfy this constraint (e.g. functions based on binomials). This is for instance the case for the C^2 function $64(-x^6+3x^5-3x^4+x^3)$ or for the C^∞ function $\exp(4-\frac{1}{x}-\frac{1}{1-x})$ extended by zeroes. One may also find functions not differentiable everywhere which satisfies the convexity/concavity property. Among them, we can quote the triangle function with a peak at $\frac{1}{2}$.

4 Asymptotic convergence

The main result of this section is the proof that the λ-MST estimator is convergent (Theorem 4): its tangent direction estimation converges toward the true continuous tangent direction as the digitization step gets finer and finer. This study is restricted to the digitization of convex shapes, but the result remains valid for shapes with a finite number of inflexion points.

Before detailing the proof, we first define properly what is a discrete local estimator and what we call multigrid convergence. We recall that previous definitions of multigrid convergence (e.g. see [12]) were restricted to global geometric properties of shapes and must be adapted to local geometric properties.

In this section S is a convex shape defined in $\mathbb{R}^2$ whose boundary ∂S can be parameterized as a twice differentiable curve of continuous curvature. We denote by $\Delta_h(S)$ the digitized boundary of S for a grid step h. We relate continuous points of ∂S to discrete points of $\Delta_h(S)$: a discrete point P_h is called an *h-digitization* of a point P of ∂S iff $\|P-P_h\|_1 \leq h$ and $P_h \in \Delta_h(S)$.

Given a grid step h, a *local discrete estimator* along a digital contour is a map that associates some value in a vector space to any ot its discrete point. A *local geometric descriptor* along a curve is a map that associates some value in a vector space to any of its points.

Definition 7. *For a shape S of $\mathbb{R}^2$, a local discrete estimator $\mathcal{E}_h$ is* multigrid convergent *toward a given local geometric descriptor $\mathcal{F}$ along ∂S iff, for any decreasing sequence of grid steps (h_i) tending toward 0, for any point P of ∂S with h_i-digitizations P_{h_i}, the sequence $\mathcal{E}_{h_i}(\Delta_{h_i}(S), P_{h_i})$ converges toward $\mathcal{F}(\partial S, P)$.*

In other words, multigrid convergence ensures asymptotically: the finer the sampling, the better the estimation. The previous definition is equivalent to classical pointwise convergence of functions with the subtlety that these functions have not the same domain.

The following subsections show these results related to local multigrid convergence:

Theorem 2. *Both λ-MST and FTT estimators are multigrid convergent toward the tangent direction along the boundary of any convex shape with twice differentiable boundary and continuous curvature. An upper bound for their average rate of convergence is $O\left(h^{\frac{1}{3}}\right)$, as the grid step h tends toward 0.*

We proceed in three steps for the proof:

1. we show that maximal segments have unbounded digital length on the contour of a shape digitized with finer and finer resolution (Proposition 2).
2. the slope of a maximal segment is then proved to tend toward the tangent direction of any point it covers (Theorem 3).
3. tangent estimators based on directions of local maximal segments (λ-MST, ET, FTT) are then proved to be (multigrid) convergent (Theorem 4).

4.1 Growth of maximal segments wrt resolution

The first important step of the proof is to establish that maximal segments on digital contour have unbounded length while the resolution increases (Proposition 2). It is based on three preliminary lemmas (Lemma 1 to Lemma 3). The first lemma tells that, on the digitization of convex shapes, contour points not inside a given maximal segment are all on the same side. The second lemma indicates that any circle separating interior and exterior pixels around a maximal segment extended on both sides has a finite radius. The last lemma shows that maximums of curvature of digitized curves are inversely proportional to the radius of separating circles. These lemmas give all the elements for proving Proposition 2: should the maximal segments be bounded as the resolution increases, then separating circles would have smaller and smaller radius; consequently the curve being digitized would have maximums of curvature tending toward infinity, which is a contradiction.

Lemma 1. *Let C be a digital boundary resulting from the digitization of a convex shape S. Let $M = C_{i,j}$ be a maximal segment of C. The characteristics of its carrying digital line Z are denoted by (a, b, μ). The values of the remainder $r_Z(P) = ax - by - \mu$ at the two points just outside M, $A \equiv C_{i-1}$ and $B \equiv C_{j+1}$, have the same sign, positive when convex and clock-wise oriented.*

Proof. We suppose here that the coordinate axes are such that the maximal segment M is located in the first octant, i.e. $0 < a \leq b$ and that the digital points under M belong to S while the points above M belong to $\overline{S}$ the complementary of S. The remainder of B relatively to Z can be less or equal to -2 or greater than $|a| + |b|$. Let us suppose $r_Z(B) \leq -2$. Let us denote by Z' the result of the translation of the line Z by $(\frac{1}{2}, -\frac{1}{2})$ and by B' the point $B + (\frac{1}{2}, -\frac{1}{2})$. We have $r_{Z'}(B') = r_Z(B) \leq -2$. Let U'_1 be the upper leaning point of Z' of minimum abscissa. It is chosen as the origin of the coordinate axes. All these notations are illustrated in Figure 7.

According to Proposition 1 of [7], the system :

$$ax - by = -1, \quad y_{B'}x - x_{B'}y \geq 0, \quad 0 < x < x_{B'}$$

has at least one solution (x, y) in the digital plane. Thus there exists a point $E' = (x_{E'}, y_{E'})$ in $\overline{S}$, such that $\frac{y_{B'} - y_{U'_1}}{x_{B'} - x_{U'_1}} \geq \frac{y_{E'}}{x_{E'}}$ (since $U'_1 = (0, 0)$). In other words, the slope defined by the two points U'_1 and B' is greater than the slope defined by the two points U'_1 and E'. Moreover the three points U'_1, E' and B' have increasing abscissae. The point E' is thus below the straight line joining U'_1 and B'. The boundary of S must pass above U'_1 (in S), below E' (in $\overline{S}$) and above B' (in S). The slope configuration between these three points is thus in contradiction with the convexity of S. The hypothesis on $r_Z(B)$ is thus wrong and the value of $r_Z(B)$ is in this case greater than $|a| + |b|$. The same argument

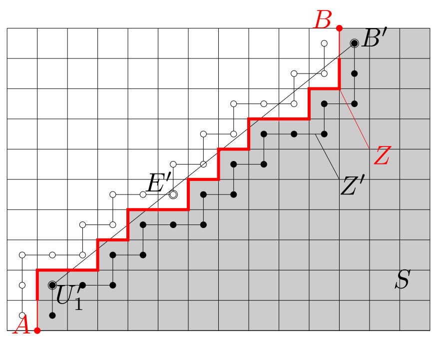

Fig. 7. This exemple can not be the digitization of a locally convex shape S. The slope defined by U'_1 and E' is lower than the slope defined by U'_1 and B', E' being outside S. The characteristics (a, b) of the digital line Z are $(5, 7)$.

can be used at the other end of the maximal segment M to prove $r_Z(A) \geq |a|+|b|$. $\square$

Lemma 2. *Let C be a digital boundary resulting from the digitization of a convex shape S. Let $M = C_{i,j}$ be a maximal segment of C. Any separating circle between the discrete points outside and inside the curve $C_{i-1,j+1}$ has a finite radius.*

Proof. We denote by Z the digital line carrying M and by (a, b, μ) its characterictics. We suppose here that M is located in the first octant, i.e. $0 < a \leq b$. According to Lemma 1, we consider the case where the value of $r_Z(P) = ax - by - \mu$ at the two points $A = C_{i-1}$ and $B = C_{j+1}$ is strictly greater than $a+b$. We will not detail the other case which is similar.

Let us denote by U an upper leaning point of M and by Z' the result of the translation of Z by $(\frac{1}{2}, -\frac{1}{2})$. Let U' be the point $U + (\frac{1}{2}, -\frac{1}{2})$, A' be $A + (-\frac{1}{2}, \frac{1}{2})$ and B' be $B + (-\frac{1}{2}, \frac{1}{2})$. These notations are illustrated in Fig. 8. We have the following properties : $A' \in \overline{S}$ and $r_{Z'}(A') = r_Z(A) \geq 1$, $B' \in \overline{S}$ and $r_{Z'}(B') = r_Z(B) \geq 1$, $U' \in S$ and $r_{Z'}(U') = 0$.

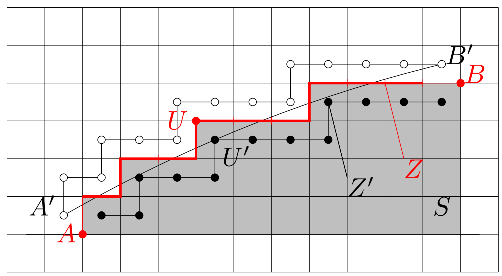

Fig. 8. Digitization of a locally convex shape S. Any separating circle between the inside and the outside has a finite radius bounded by the radius of the circumcircle through A', U' and B'.

The points A', U' and B' may not be colinear since A' and B' are strictly under the upper leaning line of Z passing through U'. They are ordered on Z'. Any circle separating the points inside and outside $C_{i-1,j+1}$ has thus a lower radius than the circumcircle defined by A', U' and B' (it has to pass below A' and B' and above U'). $\square$

Lemma 3. *Let C be the boundary of a digitized convex shape and $M = C_{i,j}$ a maximal segment of C. Any curve whose digitization contains the sequence of points $C_{i-1,j+1}$ has locally a maximum of curvature greater than $\frac{1}{r}$ where r is the radius of the separating circle of maximum radius.*

Proof. This result comes directly from Lemma 2 and from the fact that the curve traversing three non colinear given points and minimizing the curvature maximum is the circumcircle. $\square$

We are now ready to prove that maximal segments have unbounded discrete length on digitized contours as resolution increases.

Proposition 2. *Let S be a convex shape with twice differentiable contour and continuous curvature. The discrete length of the maximal segments of $\Delta_h(S)$ is not bounded while h tends towards 0.*

Proof. First of all and according to Lemma 3, two maximal segments that are equal up to an integer translation have circles of maximal radius with same radius. We consider now the set of all maximal segments of discrete length l that can be found on digitization of arbitrary convex curves. The number of maximal segments up to an arbitrary translation is clearly finite and so is the number of possible radii for circles of maximal radius according to the first remark. This number of radii being finite, we pick the greatest one and assign its inverse to the map $\kappa_1(l)$.

Interpreting Lemma 3, any digitized contour that has somewhere a maximal segment of discrete length l has also a maxima of curvature that is at least $\kappa_1(l)$ and which lies on the contour somewhere under the maximal segment.

Assume now that, whatever fine the digitization step is, some maximal segments on the digitized shape contour $\Delta_h(S)$ keep a discrete length bounded by some constant L. There is a sequence (h_i) of decreasing digitization step such that there exist some maximal segment $M_i \subset \Delta_{h_i}(S)$ with discrete length no greater than L.

Let $\kappa_{\max}(S)$ be the maxima of curvature of the boundary of S. Let $S \cdot \frac{1}{h_i}$ be the dilation of S by $\frac{1}{h_i}$. We have

$$\kappa_{\max}(S) = \frac{1}{h_i}\kappa_{\max}(S \cdot \frac{1}{h_i}) \tag{3}$$

Observing that the digitizations $\Delta_{h_i}(S)$ and $\Delta_1(S \cdot \frac{1}{h_i})$ are equivalent, we have:

$$\kappa_{\max}(S \cdot \frac{1}{h_i}) \geq \kappa_1(\mathcal{L}^1(M_i)) \tag{4}$$

$$\geq \min_{l=1}^{L} \kappa_1(l) \tag{5}$$

Denoting by $\kappa_1(1, L)$ the non-zero value $\min_{l=1}^{L} \kappa_1(l)$ and putting all together, we get:

$$\kappa_{\max}(S) \geq \frac{1}{h_i}\kappa_1(1, L) \tag{6}$$

The limit of $\kappa_{\max}(S)$ is clearly $+\infty$ when h_i tends toward 0, meaning that the contour of S has somewhere a non-bounded curvature, which is a contradiction. We may thus conclude that maximal segments have unbounded length when h tends towards 0. □

To conclude this subsection, we also examine what is the upper bound for the discrete length of maximal segments on the digitization of a circle.

Lemma 4. *Consider the digitization of step h of a circle of radius R. The discrete length of any of its DSS is upper bounded by $2^{\frac{7}{4}}(\frac{R}{h})^{\frac{1}{2}}$.*

Proof. Any digital straight line is included in a strip of thickness $2^{\frac{1}{2}}$. Hence the same holds for any digital segment on the boundary of any digitized circle. The intersection of such a strip with the circle of radius R determines an upper bound for the length of the DSS. The outer boundary of the strip is distant from the circle of $0 \leq \epsilon \leq 2^{\frac{1}{2}}$. Thus the length of the strip equals $2(2R\epsilon - \epsilon^2)^{\frac{1}{2}}$ (see Figure 9). This quantity is clearly no greater than $2(2R2^{\frac{1}{2}})^{\frac{1}{2}}$. Considering now the digitization with a grid step of h, we get that the length is upper bounded by $2(2\frac{R}{h}2^{\frac{1}{2}})^{\frac{1}{2}}$. □

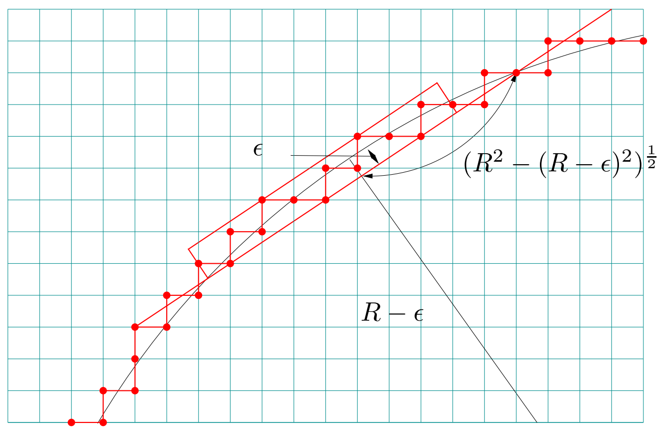

Fig. 9. A strip bounding a DSS and its intersection with a circle.

4.2 Direction of maximal segment wrt direction of tangent

We show here that maximal segments have a direction that converges to the tangent direction on the points they cover (Theorem 3). This part of the proof is mainly based on a first order Taylor expansion of the curve.

A maximal segment of $\Delta_h(S)$ is said to *cover a point P of ∂S* iff it contains a discrete point that is an h-digitization of P. For small enough h, the set of maximal segments covering P is never empty and contains the pencil of maximal segments of the point on the digitized boundary that is closest to P. The direction of maximal segments depends on the geometry of the continuous shape as follows:

Theorem 3. *Let P be a point of ∂S. The direction of any maximal segment of $\Delta_h(S)$ covering P tends towards the direction of the tangent at P while h tends towards* 0*.*

Proof. Let M_h be some maximal maximal segment covering P. We further suppose that M_h belongs to the first octant and that P is the origin of the coordinate axes. We consider the case where P is located in the left part of M_h, the other case being symmetrical. Let l be the x-coordinate of the end point of M_h of maximum abscissa. We locally parameterize the boundary $\partial S(t) = \gamma(t) = (x(t), y(t))$

as $(x, f(x))$. We denote by Q the point of ∂S with abscissa l, i.e. $Q = (l, f(l))$. See Figure 10 for an illustration of these notations.

Let $\epsilon(h)$ be the vertical thickness of M_h, i.e. the vertical distance between its two leaning lines. By definition of covering maximal segment, the distance between P and the leaning lines of M_h is at most $\epsilon(h) + h$. The same holds for Q. If p_h denotes the slope of M_h, we have:

$$\forall x \in [0, l] \quad p_h x - \epsilon(h) - h \leq f(x) \leq p_h x + \epsilon(h) + h. \tag{7}$$

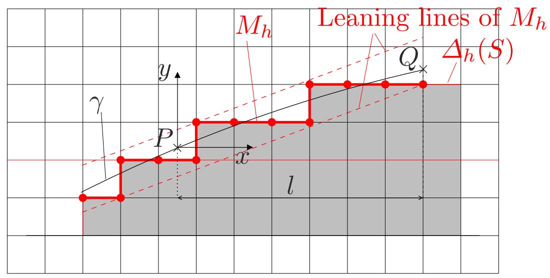

Fig. 10. Notations used in Theorem 3.

Consider that P lies on a linear part of γ, then any maximal segment covering P reaches at least one end of the linear part. Thus if D denotes the abscissa of this end of the linear part, we have:

$$\forall x \in [0, D] \quad f(x) = f'(0)x \tag{8}$$

Substituting Eq. (8) in Eq. (7), setting $x = D$ and solving it for p_h, we get:

$$f'(0) - \frac{\epsilon(h) + h}{D} \leq p_h \leq f'(0) + \frac{\epsilon(h) + h}{D}$$

Using $0 < \epsilon(h) \leq 2h$ leads to:

$$f'(0) - \frac{3h}{D} \leq p_h \leq f'(0) + \frac{3h}{D}$$

Which gives the asymptotic relation $\lim_{h \to 0} p_h = f'(0)$ for linear parts.

We now focus on non linear part where, according to Taylor's relation, we have:

$$f(l) = lf'(0) + O(l^2) \tag{9}$$

From Equations (9) and (7) we get:

$$p_h l - \epsilon(h) - h \leq lf'(0) + O(l^2) \leq p_h l + \epsilon(h) + h \Leftrightarrow p_h = f'(0) \pm \frac{\epsilon(h) + h}{l} + O(l)$$

If we denote by $L(M_h)$ the discrete length of M_h (i.e. its number of steps), the position of point Q on the right side of M_h gives the bounds:

$$\frac{hL(M_h)}{4} \leq l \leq hL(M_h). \tag{10}$$

Combining the two previous relations induces:

$$p_h = f'(0) \pm 4\frac{\epsilon(h)+h}{hL(M_h)} + O(hL(M_h))$$

As $0 < \epsilon(h) \leq 2h$ and $\lim_{h\to 0} L(M_h) = +\infty$ (Proposition 2), we have $\lim_{h\to 0} \frac{4\epsilon(h)+h}{hL(M_h)} = 0$. Since P is on a non-linear part, the boundary curve ∂S around P behaves locally as a circle of radius R. Thus using Lemma 4 and the fact that the distance d_1 and the euclidean distance are equivalent, we get $hL(M_h) = O(hR)^{1/2}$ whose limit is 0 as h tends toward 0. This entails $\lim_{h\to 0} p_h = f'(0)$.

We have just proved that the direction of M_h (slope p_h) tends toward the tangent direction at P (slope $f'(0)$) on linear and non-linear part of the shape boundary. □

4.3 Multigrid convergence of tangent estimators based on maximal segments

We are now able to prove the multigrid convergence of the λ-MST and the FTT toward the tangent direction.

Theorem 4. *Both λ-MST and FTT estimators are multigrid convergent toward the tangent direction along the boundary of any convex shape with twice differentiable boundary and continuous curvature. An upper bound for their average rate of convergence is $O\left(h^{\frac{1}{3}}\right)$, as the grid step h tends toward 0.*

Proof. Let S be such a shape, P a point on its boundary and $\theta(P)$ the tangent direction at P. Let (h_i) be any decreasing sequence of grid steps tending toward 0. We denote by P_{h_i} an h_i-digitization of P. Any maximal segment in the pencil of P_{h_i} is covering P. Consider now the λ-MST estimation at point P_{h_i}:

$$\hat{\theta}(P_{h_i}) = \frac{\sum_{j\in\mathcal{P}(P_{h_i})} \lambda(e_j(P_{h_i}))\theta_j}{\sum_{j\in\mathcal{P}(P_{h_i})} \lambda(e_j(P_{h_i}))}.$$

The direction $\hat{\theta}(P_{h_i})$ is thus a convex combination of the direction of every maximal segments containing P_{h_i}. Maximal segments in the pencil of P_{h_i} also covers P. According to Theorem 3, as i tends toward infinity, each maximal segment in the pencil of P_{h_i} has a direction tending toward $\theta(P)$. Any convex combination of values tending toward $\theta(P)$ tends also toward $\theta(P)$. The λ-MST estimator is thus multigrid convergent to the tangent direction. For the FTT estimator, it is enough to note that its direction is determined by some maximal segment in the pencil of P_{h_i}, hence a maximal segment covering P. Theorem 3 then concludes.

We may now examine the convergence speed of these estimators. From the proof of Theorem 3, the convergence speed of the direction of a maximal segment covering a point on a linear part is linear with respect to the grid step. Using the same notations as earlier-on we have for non linear parts:

$$p_h = f'(0) \pm 4\frac{\epsilon(h) + h}{hL(M_h)} + O(hL(M_h))$$

Since $h \leq \epsilon(h) \leq 2h$, the convergence speed is at least as fast as that of $\frac{1}{L(M_h)}$. The average discrete length of maximal segments on digitizations of smooth shapes has been tackled in [5] and is shown to be no slower than $\Theta\left(h^{\frac{-1}{3}}\right)$ and no faster than $\Theta\left(h^{\frac{-1}{3}} \log \frac{1}{h}\right)$. This in turn entails that the average convergence speed of the maximal segment direction is upper bounded by $O(h^{\frac{1}{3}}) + O(h^{\frac{2}{3}} \log \frac{1}{h}) = O(h^{\frac{1}{3}})$. $\square$

Experiments confirm the growth of maximal segments, as exemplified in Figure 11: they grow on average like $h^{\frac{1}{3}}$, no one has a finite length but no one grows faster than $h^{\frac{1}{2}}$. Other experiments confirm the convergence of the λ-estimator. The observed convergence speed seems even faster for this estimator on particular curves as shown on Figure 12.

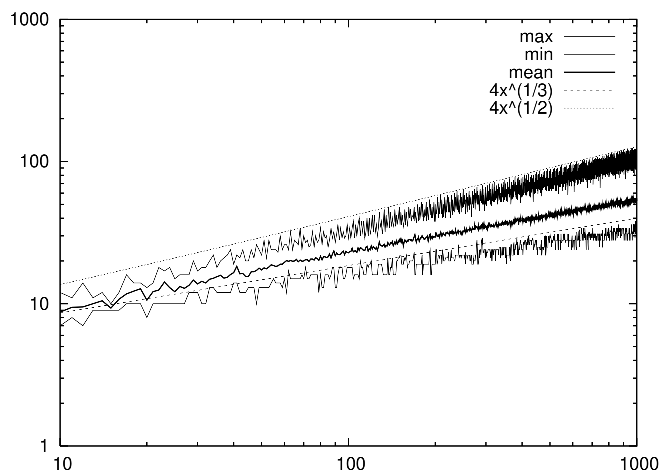

Fig. 11. Plot in log-space of the $\mathcal{L}^1$-size of maximal segments. The digitized shape is a disk of radius 1 and the abscissa is the inverse of the grid step.

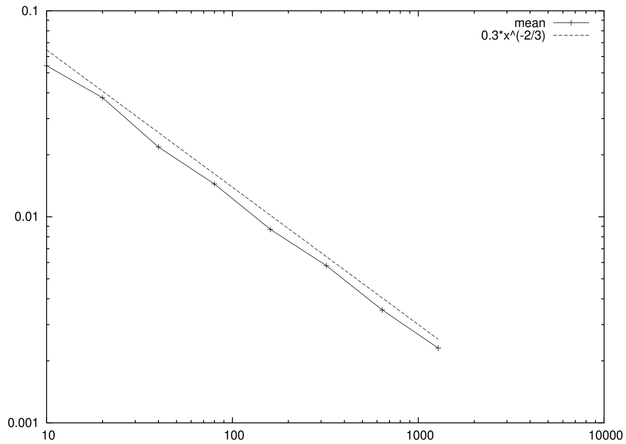

Fig. 12. Plot in log-space of the absolute deviation between the estimated tangent direction using λ-MST and the theoretical one. The digitized shape is a disk of radius 1 and the abscissa is the inverse of the grid step. The convergence speed on this shape is likely to be in $\Theta(h^{\frac{2}{3}})$.

5 Complexity of tangent estimation

We show here that the computation time of the λ-MST for all the points of a curve depends linearly on the number of points. The λ-MST estimator is thus a discrete tangent estimator with better results than the others, particularly at low scale (see Section 6 for experimental results), while keeping a computation time of the same order. One can refer to Feschet and Tougne algorithm [10] that computes the FTT along an 8-connected curve in linear time. Their algorithm is based on a $O(1)$ algorithm to remove a point to an 8-connected line segment. Moreover it finds point sequences where all points have the same tangent value which decreases the number of necessary tangent computations.

The λ-MST computation is based on an incremental update of the maximal segment M^{k+1} from the preceding maximal segment M^k. This process is efficient because adding or removing a point to a DSS can be done in constant time. This will be detailed in the following so as to provide the information needed to implement the tangent computation.

Given a maximal segment $M^k = C_{m_k,n_k}$, its next maximal segment can be defined as $C_{B(n_k+1),F(B(n_k+1))}$. It is the maximal segment containing the point n_k+1 and obtained from M^k with a minimal number of operations (adding and removing a point). The following algorithm computes it:

```
Compute_next_maximal_segment (C, M^k = C_{m_k,n_k})
   first ← m_k + 1    // removal of C^first (O(1) from Theorem 5)
   last ← n_k + 1
   while ¬S(first, last)
       first ← first + 1   // removal of C^first (O(1) from Theorem 5)
   while S(first, last)
       last ← last + 1   // addition of C^last (O(1) from Theorem 5)
   return M^{k+1} = C_{first,last−1}
```

Its principle is to remove points at the backward extremity of M^k until it becomes possible to extend the resulting segment at the other end. Of course, the characteristics of the intermediate DSS must be updated at each removal or addition of a point. The time complexity of the preceding function depends on the complexity of the updates, which are proved to be $O(1)$ by:

Theorem 5. *Assume $S(i,j)$, and assume the characteristics $D(i,j)$ of the corresponding DSS are known. Then,*

1. (Addition of point C_i or C_j) - *Deciding $S(i,j+1)$ or $S(i-1,j)$ are $O(1)$ operations and, when appropriate, computing $D(i,j+1)$ or $D(i-1,j)$ are $O(1)$ operations too (proved by Debled-Renesson and Réveillès [7]);*
2. (Removal of point C_i or C_j) - *Computing $D(i+1,j)$ or $D(i,j-1)$ are $O(1)$ operations (see below).*

An immediate corollary is that all the maximal segments of a given closed digital curve are computed with a linear complexity (each point of the curve is added once to a segment and removed once). The λ-MST can thus be computed for all the curve points in linear time : once the maximal segments are computed, the tangent direction at each point is a weighted sum of n directions of maximal segments. We have experimentally established that the pencil of a given point contains at most 7 maximal segments. More precisely, the experiment was run on circles of increasing radii inferior to 16000. For standard images, this number is thus bounded. On average, a point belongs to 3.5 maximal segments.

We now explain briefly how to update a DSS in constant time when removing a point to prove point 2 of Theorem 5. Let $C_{i,j}$ be a DSS of characteristics $D(i,j) = (a, b, \mu, U_m, U_M, L_m, L_M)$. Without any loss in generality we suppose that the digital segment $C_{i,j}$ belongs to the first quadrant. In the following, we denote by $(a', b', \mu', U'_m, U'_M, L'_m, L'_M)$ the characteristics $D(i+1,j)$ of the DSS $C_{i+1,j}$, which we wish to compute. Our algorithm is based on the observation that if the addition of the point C_i to $C_{i+1,j}$ has changed the characteristics $D(i+1,j)$, its removal from $C_{i,j}$ should do an inverse modification to $D(i,j)$.

We have first to recall how the characteristics of a DSS are updated when a point is added according to Debled's incremental algorithm [7]. When adding the point C_i to the DSS $C_{i+1,j}$, three cases may appear:

(1) C_i is in between the leaning lines: the characteristics do not change.
(2) C_i is just over the upper leaning line ($a'x_{C_i} - b'y_{C_i} = \mu' - 1$): the slope decreases and the characteristics have to be updated.

(3) C_i is just under the lower leaning line ($a'x_{C_i} - b'y_{C_i} = \mu' + a' + b'$): the slope increases and the characteristics have to be updated.

In case (2), the characteristics are updated as follows :

$$(a, b, \mu, U_m, U_M, L_m, L_M) = (y_{U'_M} - y_{C_i}, x_{U'_M} - x_{C_i}, ax_{U'_M} - by_{U'_M}, C_i, U'_M, L'_m, L'_m)$$

See Figure 13 for an illustration. We will not detail case (3) which is similar.

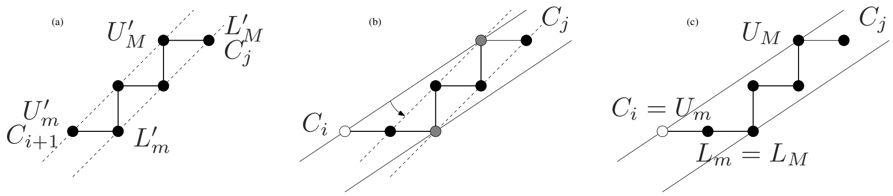

Fig. 13. Addition of a point to a DSS. (a) DSS $C_{i+1,j}$. (b) The point C_i is just over the upper leaning line and its addition will decrease the segment slope. The update can be interpreted as a rotation of the leaning lines around the pivot points U'_M and L'_m (in gray). (c) DSS $C_{i,j}$. Its slope and the leaning points U_m and L_M have to be recomputed.

If the addition of the point C_i to $C_{i+1,j}$ has changed the DSS characteristics, then C_i is an upper or lower leaning point of $C_{i,j}$. Fig. 14 illustrates the case where C_i is an upper leaning point that is being removed from the DSS.

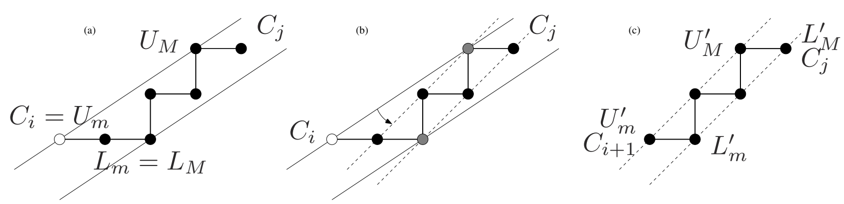

Fig. 14. Removal of a point from a DSS. (a) DSS $C_{i,j}$. The point C_i is an upper leaning point and its removal will increase the segment slope. (b) Rotation of the leaning lines around the pivot points (in gray) during the removal of C_i. (c) DSS $C_{i+1,j}$. Its slope and the leaning points U'_m and L'_M have to be recomputed.

More precisely in this case ($C_i = U_m$), the addition algorithm indicates that the slope has changed iff $\overrightarrow{C_iU_M} = (b, a)$ and $L_m = L_M$. Clearly, the addition of C_i to $C_{i+1,j}$ has decreased the slope of the DSS. Geometrically, the addition corresponds to a rotation of the upper leaning line around U'_M and of the lower leaning line around L'_m. The two leaning points U_M and L_m are thus left unchanged by the removal of C_i. We can also easily state that the point

$P = (x_{C_i}+1, y_{C_i}-1)$ would have extended $C_{i+1,j}$ without modifying its characteristics $D(i+1,j)$. The values (a', b', μ') are deduced from P. Updating of U_m and L_M is a little more tricky and exploits the property that the vector linking two successive upper (or lower) leaning points is (b', a'). The computation of the characteristics $D(i+1,j)$ are summed up in the first column of Table 1. Its second column corresponds to the case where C_i is a lower leaning point and its removal decreases the slope.

	$C_i = U_m \wedge \overrightarrow{C_i U_M} = (b,a) \wedge L_m = L_M$	$C_i = L_m \wedge \overrightarrow{C_i L_M} = (b,a) \wedge U_m = U_M$
a'	$y_{L_m} - (y_{C_i} - 1)$	$y_{U_m} - (y_{C_i} + 1)$
b'	$x_{L_m} - (x_{C_i} + 1)$	$x_{U_m} - (x_{C_i} - 1)$
μ'	$a' x_{U_M} - b' y_{U_M}$	$a' x_{U_m} - b' y_{U_m}$
U'_m	$U_M - \left\lfloor \frac{x_{U_M} - x_{C_i} - 1}{b'} \right\rfloor (b', a')$	U_m
U'_M	U_M	$U_m + \left\lfloor \frac{y_{C_j} - y_{C_i} - 1}{a'-1} \right\rfloor (b', a')$
L'_m	L_m	$L_M - \left\lfloor \frac{y_{L_M} - y_{C_i} - 1}{a'} \right\rfloor (b', a')$
L'_M	$L_m + \left\lfloor \frac{x_{C_j} - x_{C_i} - 1}{b'-1} \right\rfloor (b', a')$	L_M

Table 1. Updates of $D(i,j)$ when removing point C_i.

We have shown that the computation time of the λ-MST for all the points of a curve depends linearly on the number of points. The tangent can also be computed at only one point C_k of a given curve. The complexity of the tangent computation from this local point of view is equivalent to the complexity of computing the pencil $\mathcal{P}(k)$ around C_k. It depends on the local shape of the curve $(O(F(k) - B(k)))$.

6 Experimental evaluation

In this section, we perform a quantitative evaluation of tangent estimators based on DSS recognition. The behaviour of the λ-MST estimator relies on the λ function which monitor the estimation of the underlying curve. For example recontructing C^∞ functions requires C^∞ λ functions. We choose to minimize the curvature of the underlying curve by taking the symmetric triangle function with a peak at $\frac{1}{2}$ as λ function. This function estimates the continuous underlying curve as a circular arc when the pencil of maximal segments is reduced to two maximal segments. Moreover it gives very good practical results. In the computer implementation, all tangent directions are estimated wrt linels, not points (i.e. geometric quantities are computed at curvilinear abscissa $k + \frac{1}{2}$ and all DSS includes k and $k+1$).

We first compare the behavior of tangent estimators on smooth and flat parts and on corners. The shape is a circle in three quadrants and a right angle in the fourth (see “rsquare” in Fig. 15). Fig. 16 displays (a subset of) the estimations of the tangent direction. Estimators that satisfies the convexity/concavity property,

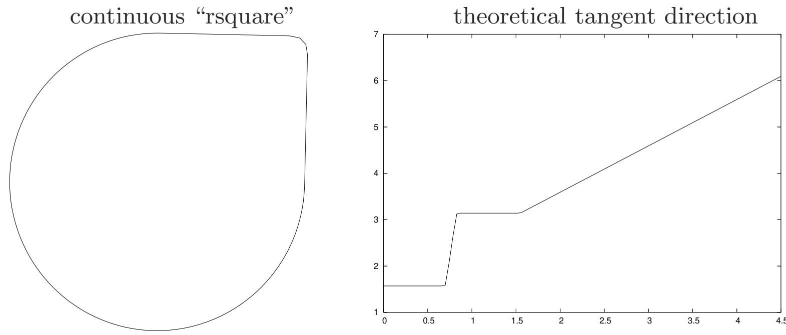

Fig. 15. The real "rsquare" shape (left) and the corresponding theoretical tangent direction (right).

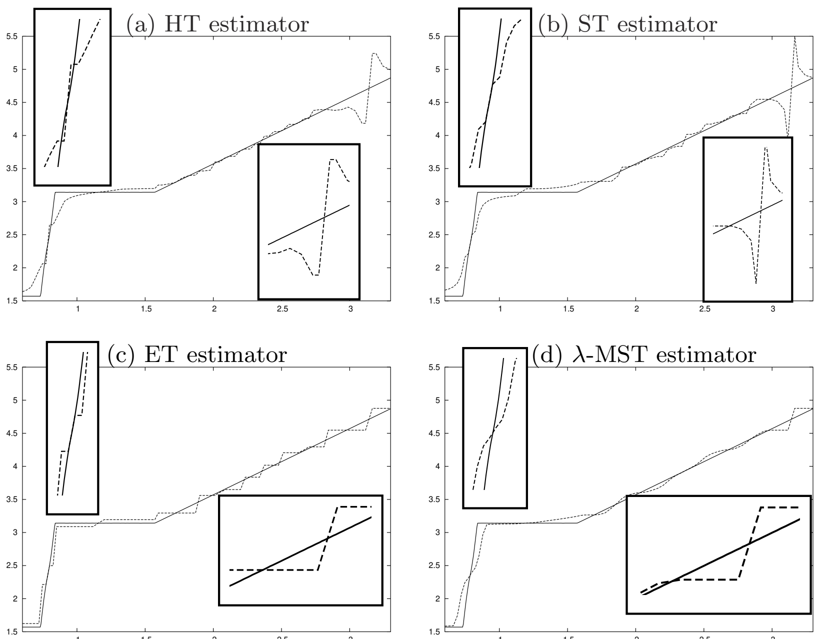

Fig. 16. Plots of the estimated tangent direction as a function of the polar angle. The shape is a circle of radius 10 with a sharp corner in the first quadrant. Solid lines correspond to expected values, dashed lines to estimations with a grid step of 0.5, dotted lines to estimations with a finer grid step of 0.25.

i.e. ET and λ-MST, create a non-decreasing sequence of directions. ST and HT clearly fail, especially at points where the digital contour meets a quadrant change. Most estimators behave correctly at corners. λ-MST slightly smoothes the corner at low resolution. The tendency to polygonalize the curve of ET (and thus FTT) appears clearly on Fig. 16c.

We then evaluate the anisotropy of the estimators with the experiment described in Fig. 17. The λ-MST is more isotropic than the others, with a steady and low mean and maximal error.

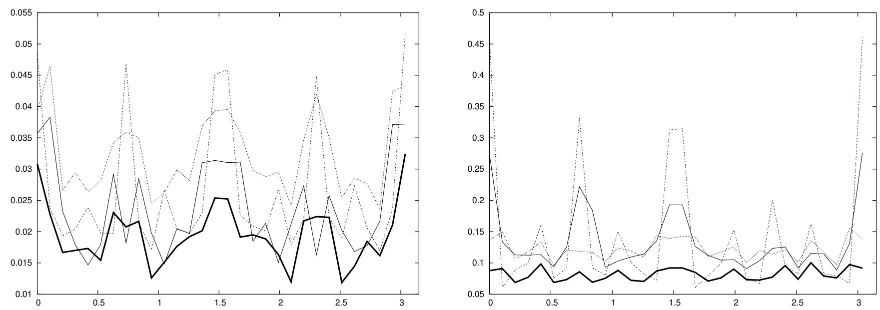

Fig. 17. Isotropy of tangent estimators measured with absolute error $|\hat{\theta}(t) - \theta(t)|$ (thick solid line: λ-MST, thin solid line: HT, dashed line: ST, dotted line: ET). Left: mean of absolute error. Right: Maximum of absolute error. For each estimator, 100 experiments are run on a circle of radius 50 with a center arbitrarily shifted in its pixel. The absolute error is drawn as a function of the polar angle and gathered by sectors of $\frac{5}{180}\pi$.

We finally examine the asymptotic behavior of the absolute error for different shapes on Table 2. Both λ-MST and ET have an asymptotic convergence in mean and in maximum. The maximum error of ST and HT cannot converge toward 0 for arbitrary shapes as shown in [14]. Although the λ-MST is not always the best in mean at coarse resolution, it has the fastest asymptotic convergence in mean and in maximum whatever the shape is.

7 Conclusions

In this paper, we have compared several tangent estimators based on DSS recognition. After a first qualitative analysis, we have proposed a new estimator which takes the best out of the existing ones. We have first checked that it satisfies the convexity/concavity property: it does not create false inflexion points along digitized shapes. Then we have proved that this tangent estimator is multigrid convergent and we have exhibited an upper bound for the average speed of convergence. We have shown too how to compute it efficiently in optimal time wrt to input data. After experimental evaluation, the λ-MST appears to be the most robust tangent estimator and very often the most accurate. The results are summed up in Table 3. Future work will focus on curvature estimators based on maximal segments and their properties.

References

1. I.M. Anderson and J.C. Bezdek. Curvature and tangential deflection of discrete arcs: a theory based on the commutator of scatter matrix pairs and its application to vertex detection in planar shape data. *IEEE Transactions on Pattern Analysis and Machine Intelligence*, 6:27–40, 1984.
2. D. Coeurjolly. *Algorithmique et géométrie discrète pour la caractérisation des courbes et des surfaces*. PhD thesis, Université Lumière Lyon 2, France, 2002.
3. D. Coeurjolly and R. Klette. A comparative evaluation of length estimators of digital curves. *IEEE Transactions on Pattern Analysis and Machine Intelligence*, 26(2):252–258, 2004.
4. D. Coeurjolly and O. Teytaud. Multigrid convergence of discrete differential estimators: Discrete tangent and length estimation. Technical Report 0101, Laboratoire ERIC, Université Lumière - Lyon 2, France, 2001.
5. F. de Vieilleville and J.-O. Lachaud. New bounds on the number and length of maximal segments on a convex digital polygon. Research Report 1364-05, LaBRI, University Bordeaux 1, Talence, France, 2005.
6. F. de Vieilleville, J.-O. Lachaud, and F. Feschet. Maximal digital straight segments and convergence of discrete geometric estimators. In *Proc. 14th Scandinavian Conference on Image Analysis (SCIA'2005), Joensuu, Finland*, volume 3540 of *LNCS*, pages 988–1003. Springer, 2005.
7. I. Debled-Renesson and J.-P. Réveillès. A linear algorithm for segmentation of discrete curves. *International Journal of Pattern Recognition and Artificial Intelligence*, 9:635–662, 1995.
8. I. Debled-Rennesson, J.-L. Rmy, and J. Rouyer-Degli. Detection of discrete convexity of polyominos. *Discrete Applied Mathematics*, 125:115–133, 2003.
9. Chul E.Kim. Digital convexity, straightness, and convex polygons. *IEEE Trans. on Pattern Anal. and Machine Intell.*, 6(6):618–626, 1982.
10. F. Feschet and L. Tougne. Optimal time computation of the tangent of a discrete curve: Application to the curvature. In *Proc. DGCI'99*, volume 1568 of *LNCS*, pages 31–40. Springer, 1999.
11. F. Feschet and L. Tougne. On the min dss problem of the closed discrete curves. *Discrete Applied Mathematics*, 2004. Accepted for publication.
12. R. Klette and J. Žunić. Multigrid convergence of calculated features in image analysis. *Journal of Mathematical Imaging and Vision*, 13:173–191, 2000.
13. V. Kovalevsky and S. Fuchs. Theoretical and experimental analysis of the accuracy of perimeter estimates. In Förster and Ruwiedel, editors, *Proc. Robust Computer Vision*, pages 218–242, 1992.
14. J.-O. Lachaud. On the convergence of some local geometric estimators on digitized curves. Research Report 1347-05, LaBRI, University Bordeaux 1, Talence, France, 2005.
15. J.-O. Lachaud and A. Vialard. Discrete deformable boundaries for the segmentation of multidimensional images. In *Proc. 4th Int. Workshop on Visual Form*, volume 2059 of *LNCS*, pages 542–551. Springer, 2001.
16. J.-O. Lachaud and A. Vialard. Geometric measures on arbitrary dimensional digital surfaces. In *Proc. DGCI'03*, volume 2886 of *LNCS*, pages 434–443. Springer, 2003.
17. J.-O. Lachaud, A. Vialard, and F. de Vieilleville. Analysis and comparative evaluation of discrete tangent estimators. In E. Andrès, G. Damiand, and P. Lienhardt, editors, *Proc. Int. Conf. Discrete Geometry for Computer Imagery (DGCI'2005), Poitiers, France*, volume 3429 of *LNCS*, pages 140–251. Springer, 2005.

18. A. Lenoir, R. Malgouyres, and M. Revenu. Fast computation of the normal vector field of the surface of a 3D discrete object. In *Proc. DGCI'96*, volume 1176 of *LNCS*, pages 101–112. Springer, 1996.
19. J. Matas, Z. Shao, and J. Kittler. Estimation of curvature and tangent direction by median filtered differencing. In *Proc. of 8th International Conference on Image Analysis and Processing*, pages 83–88, 1995.
20. H. Reiter-Doerksen and I. Debled-Rennesson. Convex and concave parts of digital curves. In *Dagstuhl Seminar "Geometric Properties from Incomplete Data"*, March 2004.
21. J.-P. Réveillès. *Géométrie discrète, Calcul en nombres entiers et algorithmique.* PhD thesis, Université Louis Pasteur, Strasbourg, France, 1991.
22. A. Vialard. Geometrical parameters extraction from discrete paths. In *Proc. DGCI'96*, volume 1176 of *LNCS*, pages 24–35. Springer, 1996.
23. M. Worring and A. W. M. Smeulders. Digital curvature estimation. *CVGIP: Image Understanding*, 58:366–382, 1993.

A Proof of Theorem 1

We show here a necessary and sufficient condition for the λ function to define a λ-MST tangent estimator satisfying the convexity/concavity property.

Theorem 1. *If λ is differentiable on $]0,1[$, then the λ-MST estimator satisfies the convexity/concavity property iff $\frac{d}{dt}(t\frac{\lambda'}{\lambda}(t)) \leq 0$ and $\frac{d}{dt}((1-t)\frac{\lambda'}{\lambda}(t)) \leq 0$ hold on this interval.*

These two conditions once put together entail λ is necessarily log-concave (i.e. $\ln\lambda$ is a concave function or $\frac{d^2}{dt^2}(\ln\lambda(t)) \leq 0$). Furthermore, it is enough to check $\frac{d}{dt}(t\frac{\lambda'}{\lambda}(t)) \leq 0$ for functions symmetric around $\frac{1}{2}$.

Proof. We first rewrite $\hat{\theta}'(k)$ as

$$\frac{\sum_{i<j}(\theta_i-\theta_j)\left(\frac{\lambda(e_j(k))\lambda'(e_i(k))}{L_i} - \frac{\lambda(e_i(k))\lambda'(e_j(k))}{L_j}\right)}{(\sum_j \lambda(e_j(k)))^2}. \tag{11}$$

We assume for instance that the angles (θ_i) of the segment in the pencil around k are nondecreasing. We must thus prove $\hat{\theta}'(k)$ is nonnegative, whatever is the curve under examination. Since some curves have points with exactly two maximal segments going through, Eq. (11) may be reduced to one pair. It is thus necessary to show that each term of this sum is nonnegative. It is also a sufficient condition. Otherwise said, we have to prove for any $i < j$,

$$\forall k, m_j < k < n_i, \frac{\lambda(e_j(k))\lambda'(e_i(k))}{L_i} - \frac{\lambda(e_i(k))\lambda'(e_j(k))}{L_j} \leq 0. \tag{12}$$

Let $R_{ij} = n_i - m_j$ be the size of the common part of both segments. Setting $t = \frac{k-m_j}{R_{ij}}$, we define two analogs of the eccentricities $e_i(k)$ and $e_j(k)$ as $\epsilon_i(t) =$

$e_i(k) = 1 - \frac{R_{ij}}{L_i}(1-t)$ and $\epsilon_j(t) = e_j(k) = \frac{R_{ij}}{L_j}t$. Eq. (12) is then equivalent to

$$\forall t \in]0,1[, \qquad \lambda(\epsilon_j(t))\frac{\lambda'(\epsilon_i(t))}{L_i} \leq \lambda(\epsilon_i(t))\frac{\lambda'(\epsilon_j(t))}{L_j} \tag{13}$$

$$\Leftrightarrow \frac{R_{ij}}{L_i}\frac{\lambda'}{\lambda}(\epsilon_i(t)) \leq \frac{R_{ij}}{L_j}\frac{\lambda'}{\lambda}(\epsilon_j(t)) \Leftrightarrow \frac{d}{dt}(\ln\lambda(\epsilon_i(t))) \leq \frac{d}{dt}(\ln\lambda(\epsilon_j(t))) \tag{14}$$

It is easy to see that $\epsilon_i(t) > t > \epsilon_j(t)$ which gives the idea to break Eq. (14) in two parts as follows, for all $t \in]0,1[$:

$$\frac{d}{dt}(\ln\lambda(\epsilon_i(t))) \leq \frac{d}{dt}(\ln\lambda(t)) \text{ and } \frac{d}{dt}(\ln\lambda(t)) \leq \frac{d}{dt}(\ln\lambda(\epsilon_j(t))) \tag{15}$$

Eq. (15) clearly implies Eq. (14), but the converse is also true by letting L_i or L_j tend toward R_{ij}.

We focus on the right part of Eq. (15). Letting $\delta = \frac{R_{ij}}{L_j}$ and $f = \ln\lambda$, we get

$$\forall\delta, 0 < \delta < 1, \frac{d}{dt}(f(t)) \leq \frac{d}{dt}(f(\delta t)), \text{ otherwise said } f'(t) \leq \delta f'(\delta t). \tag{16}$$

We now show that Eq. (16) is equivalent to

$$\frac{d}{dt}(tf'(t)) \leq 0. \tag{17}$$

Indeed, integrating both terms of the last inequality between δt and t shows sufficiency. It is also necessary since Eq. (16) can be rewritten with $h = (1-\delta)t$ as:

$$f'(t) \leq (1 - \frac{h}{t})f'(t-h) \tag{18}$$

$$\frac{f'(t) - f'(t-h)}{h} + \frac{f'(t-h)}{t} \leq 0 \tag{19}$$

Getting the limit when h tends toward 0 and multiplying both sides by t give $tf''(t) + f'(t) \leq 0$, which is exactly Eq. (17).

We now focus on the left part of Eq. (15). Letting $\delta' = \frac{R_{ij}}{L_i}$ and $g(t) = f(1-t)$, we get

$$\forall\delta', 0 < \delta' < 1, \frac{d}{dt}(f(1-\delta'(1-t))) \leq \frac{d}{dt}(f(t)), \tag{20}$$

$$\text{with } u = 1-t, \text{ we have } -\frac{d}{du}(f(1-\delta' u)) \leq -\frac{d}{du}(f(1-u)), \tag{21}$$

$$\text{or } \frac{d}{du}(g(u)) \leq \frac{d}{du}(g(\delta' u)), \text{ otherwise said } g'(u) \leq \delta' g'(\delta' u). \tag{22}$$

From the preceding paragraph, we deduce that $\frac{d}{du}(ug'(u)) \leq 0$. Since $g'(u) = -f'(1-u)$, we get

$$\frac{d}{dt}((1-t)f'(t)) \leq 0, \tag{23}$$

which concludes the proof. □

		circle 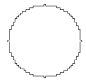				flower 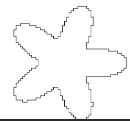				rsquare 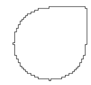			
		HT	ET	ST	λ-MST	HT	ET	ST	λ-MST	HT	ET	ST	λ-MST
mean error	$\frac{1}{10}$	0.0624	0.0830	0.0665	0.0541	0.1736	0.1364	0.1258	0.1541	0.0734	0.0876	0.0834	0.0529
	$\frac{1}{20}$	0.0411	0.0565	0.0443	0.0378	0.1050	0.0868	0.0756	0.0881	0.0501	0.0572	0.0560	0.0344
	$\frac{1}{40}$	0.0265	0.0367	0.0295	0.0218	0.0621	0.0561	0.0487	0.0519	0.0328	0.0357	0.0368	0.0194
	$\frac{1}{80}$	0.0174	0.0236	0.0185	0.0144	0.0364	0.0369	0.0311	0.0293	0.0204	0.0220	0.0220	0.0127
	$\frac{1}{160}$	0.0115	0.0152	0.0120	0.0086	0.0209	0.0232	0.0190	0.0165	0.0130	0.0137	0.0137	0.0080
	$\frac{1}{320}$	0.0077	0.0098	0.0079	0.0057	0.0128	0.0151	0.0123	0.0098	0.0081	0.0087	0.0084	0.0052
	$\frac{1}{640}$	0.0049	0.0062	0.0049	0.0035	0.0078	0.0095	0.0075	0.0059	0.0052	0.0054	0.0052	0.0032
maximum error	$\frac{1}{10}$	0.5432	0.3887	0.7700	0.2934	1.2836	1.4821	1.2415	1.4821	0.5228	0.3858	0.7496	0.2880
	$\frac{1}{20}$	0.5267	0.2695	0.7840	0.1997	1.1753	1.2028	0.9831	1.1705	0.5201	0.2903	0.7775	0.1775
	$\frac{1}{40}$	0.0353	0.0455	0.0383	0.0306	0.8760	0.9690	0.7803	0.9576	0.2871	0.2049	0.4701	0.1216
	$\frac{1}{80}$	0.2717	0.1232	0.4639	0.0770	0.7220	0.7317	0.8201	0.6496	0.2151	0.1498	0.3270	0.0832
	$\frac{1}{160}$	0.0137	0.0174	0.0142	0.0108	0.6070	0.5023	0.7796	0.3872	0.2671	0.1055	0.4645	0.0597
	$\frac{1}{320}$	0.1395	0.0592	0.2450	0.0383	0.5269	0.3312	0.7931	0.2483	0.1809	0.0763	0.3202	0.0440
	$\frac{1}{640}$	0.0935	0.0422	0.1651	0.0281	0.5018	0.2178	0.7878	0.1479	0.1359	0.0543	0.2452	0.0304
std. dev. (10^{-3})	$\frac{1}{10}$	3.0355	4.6088	4.5854	2.2948	23.13	17.58	15.205	21.56	2.5668	3.7235	3.7503	2.0155
	$\frac{1}{20}$	1.5298	2.0248	2.2530	0.9036	11.41	9.570	8.096	11.025	1.30458	1.7415	1.7463	0.8679
	$\frac{1}{40}$	0.6966	0.8301	0.9847	0.3411	5.05	4.478	4.004	4.480	0.5835	0.7531	0.7707	0.3395
	$\frac{1}{80}$	0.3139	0.3663	0.4497	0.1411	1.939	2.109	1.978	1.4257	0.2796	0.3439	0.3417	0.1488
	$\frac{1}{160}$	0.1382	0.1563	0.1885	0.0568	0.717	0.8563	0.845	0.4638	0.1224	0.1519	0.1405	0.0607
	$\frac{1}{320}$	0.0624	0.0673	0.0809	0.0247	0.296	0.3773	0.3821	0.1653	0.0616	0.0684	0.0674	0.0278
	$\frac{1}{640}$	0.0267	.0281	0.0331	0.0100	0.121	0.1561	0.1537	0.0624	0.0244	0.0286	0.0266	0.0116

Table 2. Asymptotic convergence of mean and maximum absolute error on tangent estimators and standard deviation of mean absolute error. Best value is shaded. Grid step vary from $\frac{1}{10}$ to $\frac{1}{640}$. The maximum and minimum curvatures of the shapes are "circle" : $\kappa_M = \kappa_m = 1$, "flower" : $\kappa_M \approx 5.8$, $\kappa_m \approx -26.1$, "rsquare" : $\kappa_M = 100$, $\kappa_m = 0$.

tangent estimator	straight parts	smooth parts	corners	convexity /concavity	isotropy	mean error	maximal error	point convergence
λ-MST	$+$	$+$	$=$	Yes*	$+$	$++$	$++$	Yes
HT	$=$	$+/-$	$+$	No	$-$	$+$	$-$	No
ET	$+$	$=$	$+$	Yes	$=$	$+$	$+$	Yes
ST	$=$	$+/-$	$=$	No	$-$	$+$	$-$	No

(*) For λ functions satisfying conditions of Theorem 1.

Table 3. Comparison of discrete tangent estimators. The λ-MST estimator has an average behaviour on corners and seems to be the best elsewhere.